Accurate prediction of 3D mask topography induced best focus variation in full-chip photolithography applications

Peng Liu*
Brion Technologies, Inc., an ASML company, 4211 Burton Drive, Santa Clara, CA, USA 95054

ABSTRACT

Best focus variation among different device features is one of the limiting factors to process window in semiconductor photolithography applications. Accurate prediction of best focus variation in full-chip optical proximity correction (OPC) and verifications is important in order to detect and mitigate the problem in design and post-design stages. In this work, the origin of best focus variation is first studied analytically by analyzing a simple but important imaging problem. It shows that phase difference between diffraction orders causes best focus shift. Then a rigorous simulation of mask diffraction further shows that the phase difference induced by 3D mask topography is non-zero and is a function of pattern and angle of incidence onto the mask. As a result, 3D mask models that can take into account oblique incidence effects are required in order to accurately predict best focus variations in full-chip applications. Tachyon M3D is a fast 3D mask model developed for full-chip OPC and verifications. Its accuracy in predicting best focus variation against measured wafer data is evaluated in this work. The results show very good correlation between M3D simulations and experiments.

Keywords: lithography, best focus, best focus shift, best focus variation, mask topography, 3D mask, thick mask.

1. INTRODUCTION

As semiconductor feature sizes continue to shrink, the allowable error margins for critical dimension (CD) control becomes increasingly tight due to decreased process window. One of the limiters to the process window is best focus variation among different device features, as illustrated in Figure 1. When different features have different best focus locations, the common process window is reduced even if each individual feature has a large depth of focus of its own. Therefore it is extremely important for a lithography simulator to predict this effect accurately in full-chip applications so that potential problems can be identified and corrected via optical proximity correction (OPC), source mask optimization (SMO) and other wavefront engineering methods at the design and post-design stages [1].

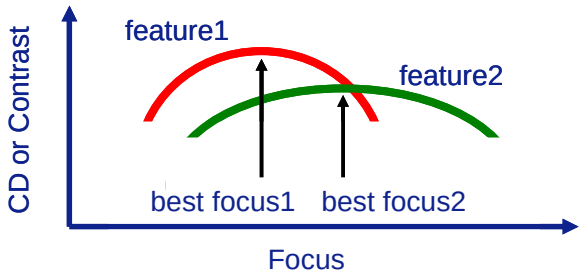

Fig.1: Illustration of best focus variation among different device features

Although the best focus can be affected by many factors, 3D mask topography is a leading cause to best focus variation among different device features [2]. 3D mask topography produces phase “errors” among diffraction orders as compared to thin mask model. These phase errors vary from feature to feature, causing best focus variation among these features.

* email: peng.liu@brion.com, phone:1-408-200-0843

Photomask Technology 2011, edited by Wilhelm Maurer, Frank E. Abboud,
Proc. of SPIE Vol. 8166, 816640 · © 2011 SPIE · CCC code: 0277-786X/11/$18 · doi: 10.1117/12.898783

Downloaded From: http://proceedings.spiedigitallibrary.org/ on 04/08/2013 Terms of Use: http://spiedl.org/terms

Oblique incidence effect also plays an important role in determining these phase errors. It should be noted that these effects are completely absent in the thin mask model of Kirchhoff approximation, therefore it cannot be used to predict the related best focus variation. Although rigorous 3D mask models based on numerical methods such as Finite Difference Time Domain (FDTD) and Rigorous Coupled Wave Analysis (RCWA) can model these effects accurately, they are computationally too expensive for full-chip applications. These applications require approximate 3D mask models that are sufficiently fast as well as capable of accurately modeling 3D electromagnetic field (EMF) scattering effects under oblique incidence.

In this paper, we first study a simple but important imaging problem analytically, which offers insight into the origin of best focus variation among device features and properties that determine the best focus. Then we discuss the modeling requirements that are essential for accurate prediction of best focus. We then describe Tachyon M3D, a fast 3D mask model developed for full-chip OPC and verification applications. We will evaluate its accuracy in predicting best focus variation among various 1D and 2D features by comparing it to experimental results.

2. AN ANALYTICAL CASE STUDY

2.1 A simple imaging problem

Figure 2 shows the problem to be analyzed in this section. It is designed to print dense 1D line/space patterns. The details of the system are described as follows.

A symmetric dipole source is employed in this system. Each pole is small enough so that it can be considered as a point source. Each point source produces a single, oblique incident planewave onto the mask. The polarization of the planewave is chosen to be transverse electric (TE) and parallel to the line/space orientation of the mask. The two point sources are considered incoherent relative to each other.

The mask pattern is dense enough so that only the 0^{th} and 1^{st} diffraction orders produced by the mask can pass through the projection lens pupil to reach the wafer.

A planar wafer filmstack is assumed in this problem so that no additional diffraction orders are produced in the resist layer by the wafer filmstack. This condition is generally met when a well-designed bottom anti-reflective coating (BARC) is used.

The above design ensures that the image produced by each of the point sources is a result of 2-beam interference in the resist. As will be shown later, it can be easily derived analytically. The final partial coherent image produced by the dipole source is simply a weighted sum of the individual images produced by the two point sources.

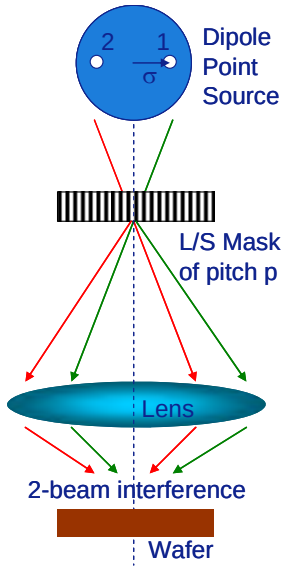

Fig.2: A system for dense 1D line/space printing applications

Although simple, this problem bears important characteristics of many practical lithography systems for dense line/space printing applications.

2.2 Image derivation

Under the condition of 2-beam interference, the total electric field produced by a point source is given by

$$E = E_0 e^{ik_0 x + i\beta_0 \Delta} + E_1 e^{ik_1 x + i\beta_1 \Delta} \tag{1}$$

$$k_0 = \frac{2\pi}{\lambda} NA\sigma \qquad k_1 = k_0 - \frac{2\pi}{p}$$

$$\beta_0 = \sqrt{\left(n\frac{2\pi}{\lambda}\right)^2 - k_0^2} \qquad \beta_1 = \sqrt{\left(n\frac{2\pi}{\lambda}\right)^2 - k_1^2}$$

Downloaded From: http://proceedings.spiedigitallibrary.org/ on 04/08/2013 Terms of Use: http://spiedl.org/terms

where λ is the wavelength of the illumination source, *NA* is the numerical aperture of the projection lens, σ is the location of the point source, *p* is the pitch of the line/space pattern, *n* is the refractive index of the wafer ambient, E_0 is the complex magnitude of the 0th diffraction order, E_1 is the complex magnitude of the 1st diffraction order, and Δ is the defocus. Note the defocus effect is modeled explicitly in the above formulation.

The image produced by the point source is therefore

$$I = |E_0|^2 + |E_1|^2 + 2|E_0||E_1|\cos[2\pi x / p + \beta\Delta - \Phi] \tag{2}$$

where $\beta=\beta_0-\beta_1$ and Φ is the phase difference between the 1st and 0th diffraction order.

The image produced by the other point source can be derived similarly. The final partial coherent image of the dipole is simply a weighted sum of the two individual images. After consideration of symmetry properties of the source and mask, the final image is given as follows and illustrated in Figure 3.

$$I = |E_0|^2 + |E_1|^2 + 2|E_0||E_1|\cos(\beta\Delta - \Phi)\cos(2\pi x / p) \tag{3}$$

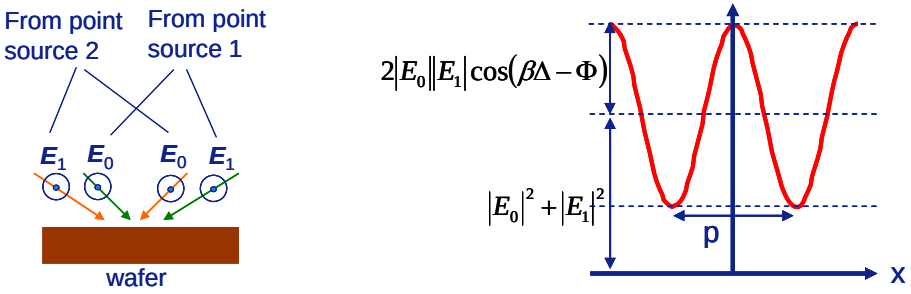

Fig.3: Illustration of partial coherent image formation by dipole point source

2.3 Interesting image properties

Some interesting image properties can be deduced from Equation 3.

2.3.1 Image contrast:

$$\frac{I_{\max} - I_{\min}}{I_{\max} + I_{\min}} = \frac{2|E_0||E_1|}{|E_0|^2 + |E_1|^2}\cos(\beta\Delta - \Phi) \tag{4}$$

2.3.2 Best focus:

$$\Delta_{BF} \equiv \frac{\Phi}{\beta} \tag{5}$$

Maximum image contrast and maximum/minimum CD are reached at the best focus.

2.3.3 Iso-focal threshold:

$$I_{th} = |E_0|^2 + |E_1|^2 \tag{6}$$

At the iso-focal threshold, CD is half of the pitch and independent of defocus.

2.3.4 Iso-focal optical condition:

$$\beta = 0 \quad \rightarrow \quad 2NA \cdot \sigma \cdot p = \lambda \tag{7}$$

Under the iso-focal optical condition, the image is independent of defocus.

Downloaded From: http://proceedings.spiedigitallibrary.org/ on 04/08/2013 Terms of Use: http://spiedl.org/terms

3. MODELING REQUIREMENTS

3.1 Contributions to phase difference

From Equation 5 of Section 2, best focus variation is proportional to the variation of phase difference between diffraction orders. Therefore accurate modeling of the phase difference is required for accurate prediction of best focus variations.

As shown in Figure 4, phase differences can be introduced at various imaging stages including mask diffraction, lens wavefront aberration and wafer filmstack. The final phase difference is the sum of all the above contributions.

$$\Phi = \Phi_{mask} + \Phi_{lens} + \Phi_{wafer} \qquad (8)$$

Modeling of the last two contributions has been well established in modern lithography simulators. This work focuses on accurate modeling of mask diffraction for full-chip applications.

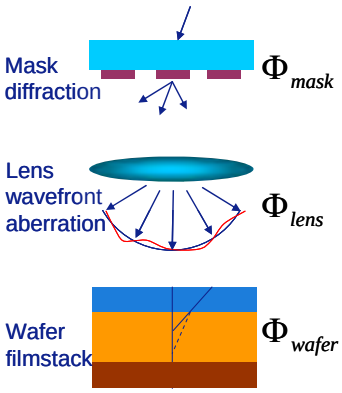

Fig.4: Contributions to phase difference

3.2 3D mask topography effects on phase difference

In this section, we show 3D mask topography induced phase differences between the 1st and 0th diffraction orders of a 6% attenuated phase shift mask (Figure 5(a)), computed using FDTD method. The mask is designed to produce 180 degree phase shift.

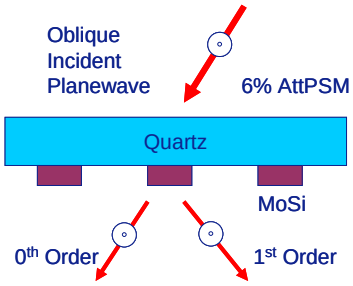

Fig. 5(a): Attenuated phase shift mask of dense line/space patterns under oblique incident illumination

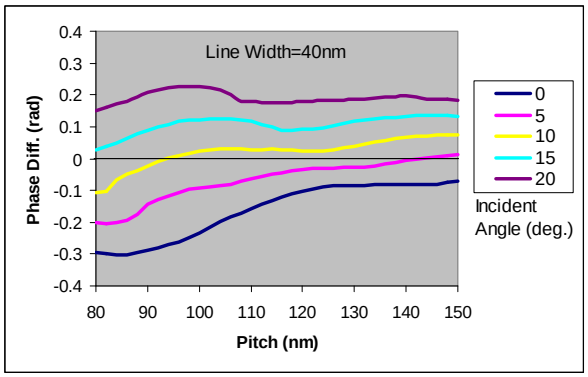

Fig. 5(b): Phase difference as a function of pitch and incident angle for MoSi line width = 40nm

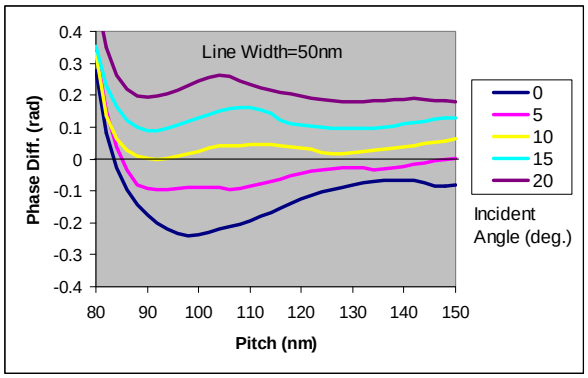

Fig. 5(c): Phase difference as a function of pitch and incident angle for MoSi line width = 50nm

3.3 Modeling requirements

As shown in Figures 5(b) and 5(c), the phase difference is non-zero and is pattern dependent, as opposed to Kirchhoff model where the phase difference is always zero for the mask of interest. In addition, the phase difference is also

Downloaded From: http://proceedings.spiedigitallibrary.org/ on 04/08/2013 Terms of Use: http://spiedl.org/terms

incident angle dependent, indicating Hopkins treatment of off-axis illumination (OAI) is not valid. The results suggest that 3D mask models that is capable of taking into account oblique incidence effects are required in order to model the phase differences and ultimately to predict the best focus variations accurately.

4. TACHYON M3D MODEL

4.1 Working principle

Tachyon M3D model is a fast, approximate 3D mask model developed for full-chip OPC and verification applications. The working principle of Tachyon M3D is illustrated in Figure 6. The details on its derivation are given in reference [3]. Note the formula can be expressed either in frequency domain as in reference [3] or in spatial domain as in this work. The later is used here because it is much easier to visualize.

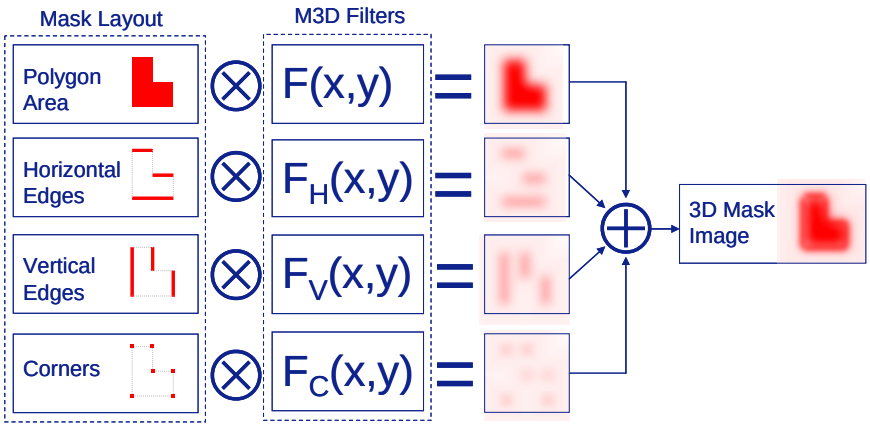

Fig. 6: Illustration of Tachyon M3D working principle

In a nutshell, a set of so-called M3D filters are used to render the mask layout into a 3D mask image that approximates the transmitted electromagnetic field of the mask.

4.2 Calculation of M3D filters

The flow chart of M3D filters calculation is shown in Figure 7. It is a 2-step process. First, a rigorous EMF solver is used to compute a set of transmitted fields on a pre-defined grid of incident angles for selected patterns of a given mask topography. Then M3D filters are extracted from the rigorous results according to the formula in Figure 6 by solving the corresponding inverse problem for a given illumination shape and polarization.

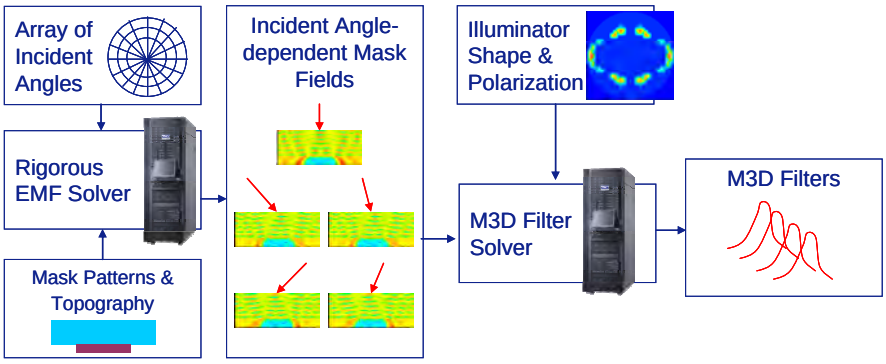

Fig. 7: Flow chart of M3D filters calculation

Once the M3D filters are obtained, they can be re-used to render 3D mask images of arbitrary mask layouts of the same mask topography.

Downloaded From: http://proceedings.spiedigitallibrary.org/ on 04/08/2013 Terms of Use: http://spiedl.org/terms

5. EXPERIMENTAL VALIDATION

In this section, we evaluate Tachyon M3D accuracy of best focus prediction against a set of experimental use cases.

5.1 Experimental best focus determination

As shown in Figure 8, to filter out measurement errors and noises, experimental focus-exposure matrix (FEM) results are fitted to a polynomial formula and the corresponding process window (PW) in elliptical form is computed. The best focus is determined by the PW center.

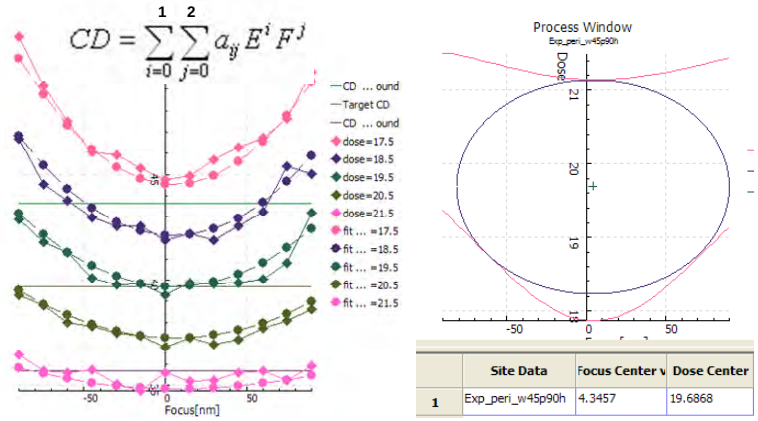

Fig. 8: Determination of experimental best focus

For consistency, simulated best focus by Tachyon is determined in the same way.

5.2 Use case #1

The first use case studies the best focus behavior of line/space patterns in various neighboring environments, including presence of scattering bars, under dipole illumination, as shown in Figure 9(a).

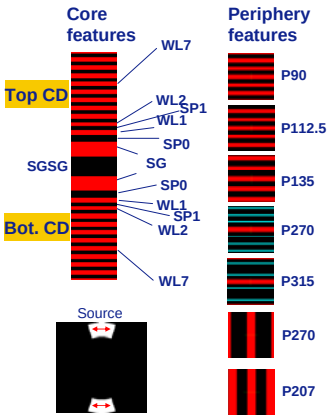

Fig. 9(a): Mask patterns

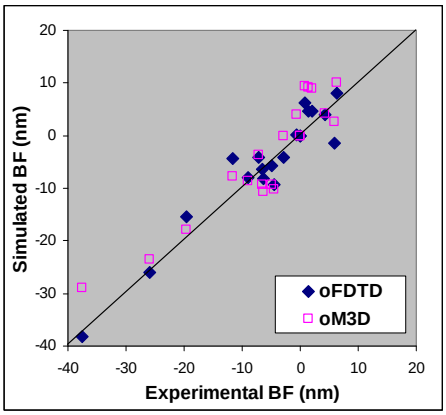

Fig. 9(b): No-Hopkins OAI treatment

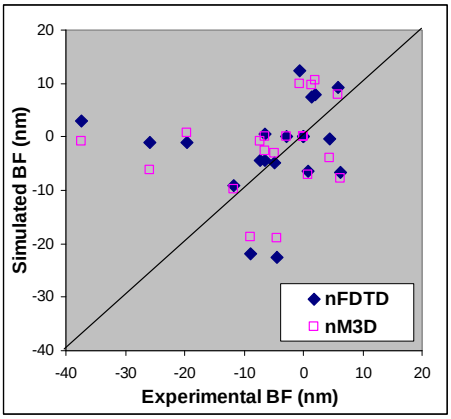

Fig.9(c): Hopkins OAI treatment

Table 1: Description of 3D mask models

3D Mask Model	Description
oFDTD	FDTD model with No-Hopkins treatment of OAI
oM3D	M3D model with No-Hopkins treatment of OAI
nFDTD	FDTD model with Hopkins treatment of OAI
nM3D	M3D model with Hopkins treatment of OAI

Downloaded From: http://proceedings.spiedigitallibrary.org/ on 04/08/2013 Terms of Use: http://spiedl.org/terms

Four different 3D mask models (as described in Table 1) are used to simulate the best focus (BF) behavior. The correlation of simulated BF to experimental BF is shown in Figure 9(b) for No-Hopkins treatment of OAI and in Figure 9(c) for Hopkins treatment of OAI. As expected from the discussion of Section 3, the correlation is good in the former case and very poor in the later.

Note, Tachyon convention of defocus sign [4] is used in all use cases presented in this work.

5.3 Use case #2

The through-pitch best focus behavior of dense line/space patterns under dipole illumination is investigated in the second use case. The results are shown in Figure 10. Again, the results show that correct treatment of oblique incidence effect in 3D mask models is important in order to predict the best focus behavior correctly. Also shown in Figure 10 is the best focus obtained by thin mask model, which is nearly pattern independent, just as expected from the discussion in Section 3.

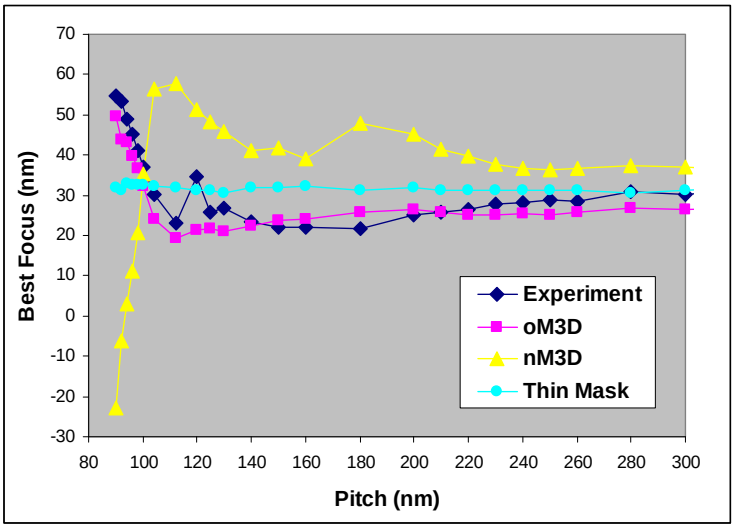

Fig. 10: Experimental and simulated best focus through pitch

5.4 Use case #3

The last use case examines the best focus behavior of 2D patterns (Figure 11(a)) under freefrom illumination (Figure 11(b)). The correlation between simulated BF and experimental BF is shown in Figure 11(c). Good correlation is obtained for the M3D model while no correlation is seen in the thin mask model.

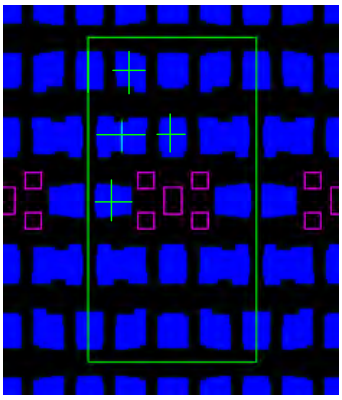

Fig. 11(a): 2D patterns

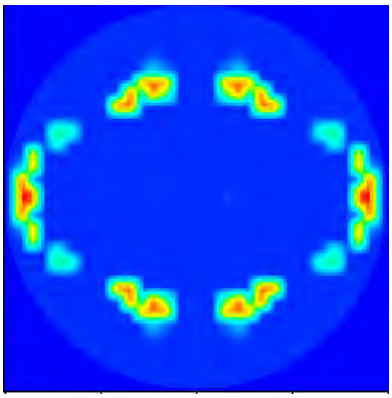

Fig. 11(b): Freeform source

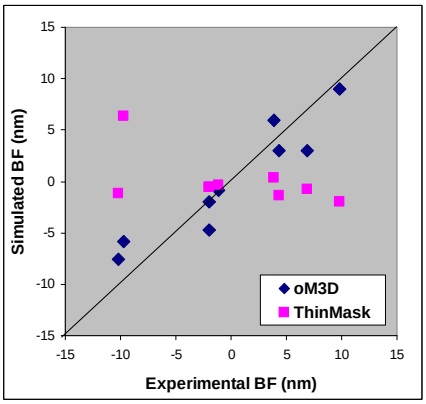

Fig. 11(c) Best focus correlation

Downloaded From: http://proceedings.spiedigitallibrary.org/ on 04/08/2013 Terms of Use: http://spiedl.org/terms

6. CONCLUSION

Through an analytical study on a simple but important imaging problem, we have established a direct relationship between the best focus and the phase difference between diffraction orders. A further study on a mask diffraction problem using a rigorous EMF solver shows that the phase difference induced by 3D mask topography is non-zero and is pattern and incident angle dependent. These studies conclude that 3D mask models that can take into account oblique incidence effects are required in order to predict best focus variation accurately. In this work, we also described Tachyon M3D, a fast 3D mask model developed for full-chip OPC and verification applications, and presented experimental validation of the model.

ACKNOWLEDGMENT

Jo Finders and Thijs Hollink of ASML for providing experimental FEM data of use case #1

Bart Laenens of IMEC (now with ASML) for providing experimental FEM data of use cases #2 & 3

Paul Van Adrichem of ASML for coordinating experimental and simulation work with IMEC

REFERENCES

[1] Frank Staals et al., “Advanced Wavefront Engineering for Improved Imaging and Overlay Applications on a 1.35 NA Immersion Scanner,” Proc. of SPIE Vol. 7973, 2011
[2] Jo Finders and Thijs Hollink, “Mask 3D effects: impact on Imaging and Placement,” 27th European Mask and Lithography Conference, Proc. of SPIE Vol. 7985, 2011
[3] Peng Liu et al., “Fast and accurate 3D mask model for full-chip OPC and verification,” Proc. of SPIE Vol. 6520, 65200R, (2007)
[4] Tachyon Model User Manual, http://www.brion.com

Downloaded From: http://proceedings.spiedigitallibrary.org/ on 04/08/2013 Terms of Use: http://spiedl.org/terms